Implementation of Image Fusion Techniques Using FPGA

M.A. Mohamed[1] and B.M. El-Den[2]
[1]Faculty of Engineering, Mansoura University, Egypt
[2]Instructor at ITC Company-Mahala, Egypt

Summary
Image fusion is a process which combines the data from two or more source images from the same scene to generate one single image containing more precise details of the scene than any of the source images. Among many image fusion methods like averaging, principle component analysis and various types of Pyramid Transforms, Discrete cosine transform, Discrete Wavelet Transform special frequency and *ANN* and they are the most common approaches. In this thesis we deal with multi-focus images. This paper addresses these issues in image fusion: Fused two images by different techniques which present in this research, Quality assessment of fused images with above methods, Comparison of different techniques to determine the best approach and Implement the best technique by using *FPGA*. First a brief review of these techniques is presented and then each fusion method is performed on various images. In addition experimental results are quantitatively evaluated by calculation of Root Mean Square Error *RMSE*, Entropy; Mean square error *MSE*, signal to noise ratio *SNR* and peak signal to noise ratio *PSNR* measures for fused images and a comparison is accomplished between these methods. Then we chose the best techniques to implement them by *FPGA*.

Keywords

Image Fusion, principal component analysis (PCA), pyramid transform, discrete wavelet transform (DWT), discrete cosine transform (DCT), FPGA.

1. Introduction

Optical lenses suffer from the problem of limited depth of field. According to the lens formula, only objects at one particular depth will be truly in focus. Consequently, if one object in the scene is in focus, another object at a different distance from the lens will be out of focus and, thus blurred. The degree of this blurring is affected by a number of factors, including the object distance, the focal length and number of the lens, and the distance between the lens and the sensor plane. One approach to achieve images in which the information content is improved and all objects are well-focused is fusing the source images. The purpose of image fusion techniques is to merge multiple images taken from the same scene with different focuses. An image fusion technique is successful to the extent that to create a composite that retains all useful information from the source images. Fusion techniques include the simplest method of pixel averaging to more complicated methods such as pyramid transform and wavelet transform. The objectives of image fusion are extracting all of the useful information from the source images without introducing artifacts or inconsistencies that will distract human observers or the following process [1, 2]. Such objectives could be achieved through creating combined images that are more suitable for human perception and computerized image processing such as augmentation, segmentation, feature extraction, and object recognition. The fused data should provide more complete information than the separate dataset does and increase reliability and accuracy to imperfection. At present, image fusion technology is widely used in various fields. Practical image fusion systems require high-speed processing, the current widespread use of software processing, and use of parallel computers to increase processing speed, but the use of parallel computer systems, there is high cost. This paper presents the image fusion technology using *FPGA*-based hardware as a design approach. Implementation for different image processing requirements, software designers can modify the *FPGA's*. Internal logic functions, *FPGA* high level of integration, so that the image fusion board more compact layout.

2. Preprocessing of Image Fusion

Two images taken in different angle of scene sometimes causes distortion. Most of objects are the same but the shapes change a little. At beginning of fusing images, we have to make sure that each pixel at correlated images has the connection between images in order to fix the problem of distortion; image registration can do this. Two images have same scene can register together using software to connect several control points. After registration, resampling is to adjust each image that about to fuse to the same dimension. After resampling, each image will be of the same size. Several interpolation approaches can be used, to resample the image; the reason is that most approaches we use are all pixel-by-pixel fused. Images with the same size will be easy for fusing process. After the resampling, fusion algorithm is applied. Sometime we have to transfer the image into different domain, sometime haven't depending on the algorithm. Inverse transfer is necessary if image has been transferred into another domain. The processes described above are denoted by preprocesses of actual fusion. Both steps are important and affect the result of fusion Fig.1.

Manuscript received May 5, 2010
Manuscript revised May 20, 2010

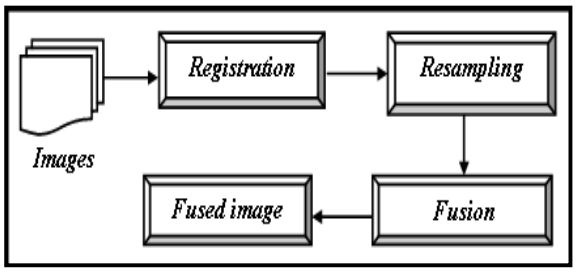

Fig.1 Generic Image Fusion Flow chart

3. Performance Evaluation of Image Fusion

Five different measures have been used to evaluate the performance of fusion process. These are: (1) information entropy; (2) means-square-error; (3) peak-signal-to-noise ratio; (4) signal-to-noise ratio, and (5) root-mean-square error.

3.1 Entropy

Entropy is one of the most important quantitative measures in digital image processing; which is defined as the quantification of information content of messages. Although used entropy in communication, it can be also employed as a measure and quantify the information content of digital images. A digital image consists of pixels arranged in rows and columns. Each pixel is defined by its position and by its grey scale level. For an image consists of L grey levels, the entropy is defined as:

$$H = -\sum_{i=1}^{L} P(i) Log_2 P(i) \quad (1)$$

where $P(i)$ is the probability of each grey scale level.

3.2 Root-Mean-Square Error (RMSE)

The root-mean-square error $RMSE$ between the reference image; I and the fused image; F, is defined as**:**

$$RMSE = \sqrt{\frac{1}{M \times N} \sum_{i-1}^{M} \sum_{j=1}^{N} [I(i,j) - F(i,j)]^2} \quad (2)$$

where i and j denotes the spatial position of pixels, while, M and N are the dimensions of the images.

3.3 Peak Signal-to-Noise Ratio (PSNR)

The peak signal-to-noise ratio $PSNR$ is the ratio between the maximum value of an image and the magnitude of background noise and is commonly used as a measure of quality of reconstruction in image fusion. It is defined in terms of the mean-squared error MSE as:

$$PSNR = 10 \log_{10} \left(\frac{(2^n - 1)^2}{MSE} \right) \quad (3)$$

where n is the number of bits per pixel of the original image I. MSE and $PSNR$ are appealing because they are simple to calculate, have clear physical meanings, and are mathematically convenient in the context of optimization, but they are not well match to perceived visual quality [4]. On the other hand, the signal-to-noise ratio SNR between the fused and the original image was calculated using the following equation:

$$SNR = 10 log_{10} \left(\frac{\sum_{i=1}^{M} \sum_{j=1}^{N} (I(i,j) - F(i,j))^2}{\sum_{i=1}^{M} \sum_{j=1}^{N} I(i,j)} \right) \quad (4)$$

where I the original image and F is the fused image

4. Image Fusion Techniques

The number of proposed concepts for image fusion is growing rapidly, which indicates ongoing research in this area. Technically, image data recorded by different sensors have to be merged or composed to generate a new representation. Alternatively, data from one sensor are also subject of image fusion. Different multispectral channels are to be considered as different sources, as well as images taken at different times by the same sensor. References for the algorithms worked out in the following are Anderson (1987); Burt (1992); Carper et al. (1990); Chavez et al. (1991); Kathleen and Philip (1994), Rockinger (1996) and Wald (2002). With respect to the conceptual approach, the proposed techniques averaging, *DCT*, *PCA*, *DWT*, Laplacian pyramid, morphological pyramid, gradient pyramid, spatial frequency and artificial neural networks .The main characteristics of these techniques are discussed in the context of its mathematical formulation.

5. Simple Approaches Fusion Techniques

5.1 Fusion Techniques based on Averaging

The simplest way to fuse two images is to take the mean-value of the corresponding pixels. Maybe that for some applications this may be enough, but there will always be one image with poor lighting and thus the quality of an averaged image will obviously decrease. Like we can see averaging doesn't actually provide very good results [4].

5.2 Principal components analysis

Principal component analysis *PCA* is a general statistical technique that transforms multivariate data with correlated variables into one with uncorrelated variables. These new variables are obtained as linear combination of the original variables.

5.2.1 Implementation

The implementation process may be summarized as: (i) Images size checking, source images must have the same size; (ii) The input images (images to be fused) are arranged in two column vectors; (iii) The resulting vector has a dimension of $n\times 2$, where n is length of the each image vector; (iv) Compute the eigenvector and eigenvalues for this resulting vector are computed and the eigenvectors corresponding to the larger eigenvalue obtained, and (v) The normalized components are computed from the obtained eigenvector; fused image is:

$$I_f(x,y)=P_1I_1(x,y)+P_2I_2(x,y) \quad (5)$$

where P_1 and P_2 are the normalized components and its equal to $P_1=V(1)\ /\ \sum V$ and $P_2=V(2)\ /\ \sum V$ where V is eigenvector and $P_1+P_2=1$.

6. Pyramid Transform Techniques

A pyramid structure can be described as a collection of images at different scales that together represent the original image. One image can be represented as a pyramid structure via pyramid transform.

6.1 Laplacian Pyramid (GP)

LP is derived from the Gaussian pyramid *GP* [3], which is a multiscale representation obtained through a recursive reduction. The first step in Gaussian pyramid coding is to low-pass filter the original image I to obtain image G_1. We say that G_1 is a "reduced" version of I in that both resolution and sample density are decreased. In a similar way we form G_2 as a reduced version of G_1, and so on. Hence, to make a fusion we flow these steps: (1) Generate *GP*; (2) *GP* interpolation; (3) Laplacian pyramid decomposition, and (4) Laplacian pyramid reconstruction. Fusion is performed in the Laplacian pyramid domain by constructing a fused pyramid. The pyramid coefficient (or hyperpixel) at each location in the fused pyramid is obtained by selecting the hyperpixel of the sensor pyramid that has the largest absolute value. Let L_A and L_B be the Laplacian pyramids of two images A and B .With L_F the fused pyramid is denoted which is determined by

$$L_F^K(i,j)=\begin{cases} L_A^K(i,j)\rightarrow & \text{if } \left|L_A^K(i,j)\right|>\left|L_A^K(i,j)\right| \\ L_B^K(i,j) & otherwise \end{cases} \quad (6)$$

where K is the level of the pyramid and *(i, j)* denotes a hyperpixel at that level.

6.2 Morphological Pyramids

The image at any level L is created by applying morphological filtering with a 3×3 structuring element to the image level *(L-1)* followed by down-sampling the filtered image with $d=2$.

6.3 Gradient Pyramids

The fusion process in gradient pyramid [5] is similar process to LP operation. By successively filtering and down sampling, an image pyramid that has the original image as the pyramid base with successive levels that are low-pass filtered and down sampled versions of the level below is generated.

7. Discrete Cosine Transform Techniques

To date, different techniques for image fusion have been presented. The simplest method is to take the average of the source images. However, this often leads to undesirable side effects including reduced contrast. Many other techniques including pyramid based image fusion and wavelet transform based image fusion have been introduced to solve this problem. This section studies image fusion in frequency domain based on the *DCT* transform. We present an image fusion technique based on average measure defined in the *DCT* domain. An improved version of direct *DCT* image fusion is obtained from the *DCT* representation of the fused image by taking the average of all the *DCT* representations of all the input images. Actually, this image fusion technique is called the *DCT + average*; modified or "improved" *DCT* technique. I can be found that, there is a contrast reduction in the fused images obtained by the modified *DCT* technique[7].

8. Discrete Wavelet Transform Techniques

The two-dimensional discrete wavelet transform is becoming one of the standard tools for image fusion. The DWT is computed by successive lowpass and highpass filtering of the digital image or images. This is called the Mallat algorithm or Mallat-tree decomposition. Its significance is in the manner it connects the continuous-time multiresolution to discrete-time filters. The principle of image fusion using wavelets is to merge the wavelet decompositions [8,9] of the two original images using fusion methods applied to approximations coefficients and details coefficients. The following two examples examine the process of image fusion to merges two different images leading to a new image: (1) Load two original images Fig.(3.1.a,b); (2) Fuse the two images from wavelet decompositions at level 5; (3) Using db2 by taking two different fusion methods; Fusion by taking the mean for both approximations and details Fig.(3.c), and (4) Fusion by taking the maximum for approximations and the minimum for the details Fig.(2.d).

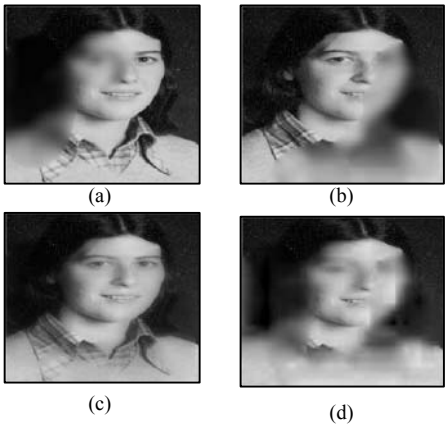

Fig.2 (a, b) original image (c) Fusion by taking the mean for both approximations and details; (d) fusion by taking the maximum for approximations and the minimum for the details

9. Spatial Frequency Techniques

9.1 Spatial frequency (SF)

Spatial frequency is used to measure the overall activity level of an image [10]. For an $M\times N$ image F, with the gray value at pixel position (m, n) denoted by $F(m, n)$, its spatial frequency is defined as

$$SF = \sqrt{RF^2 + CF^2} \tag{7}$$

where RF and CF is row frequency and column frequency:

$$RF = \sqrt{\frac{1}{MN}\sum_{m=1}^{M}\sum_{n=2}^{N}\left(F(m,n)-F(m,n-1)\right)^2} \tag{8}$$

$$CF = \sqrt{\frac{1}{MN}\sum_{n=1}^{N}\sum_{m=2}^{M}\left(F(m,n)-F(m-1,n)\right)^2} \tag{9}$$

The basic algorithm may be written as: (i) Decompose the source images into blocks of size $M\times N$; (ii) Compute the spatial frequency for each block; (iii) Compare the spatial frequencies of two corresponding blocks Ai and Bi, and construct the ith block Fi of the fused image as

$$Z_i = \begin{cases} SF_i^A & if \quad SF_i^A > SF_i^B + TH \\ SF_i^B & if \quad SF_i^A < SF_i^B - TH \\ (A_i + B_i)/2 & otherwise \end{cases} \tag{10}$$

where TH is the threshold, and (iv) Verify and correct the fusion result in step *3* with saliency checking. In this case the aim of this process is to avoid isolated blocks the process is illustrated in flow chart Fig.(3)

10. Artificial Neural Networks Techniques

PCNN is a feedback network and each *PCNN* neuron consists of three parts: the receptive field, the modulation field, and the pulse generator [11]. *PCNN* in image fusion is a single layer pulse coupled neural cells with a two-dimensional connection as shown in Fig.4 [12, 13]. In this section, we introduce an image fusion method based on *PCNN* network. The implementation is computationally simple and can be realized in real-time. Fig.5 shows a schematic diagram of the proposed image fusion method

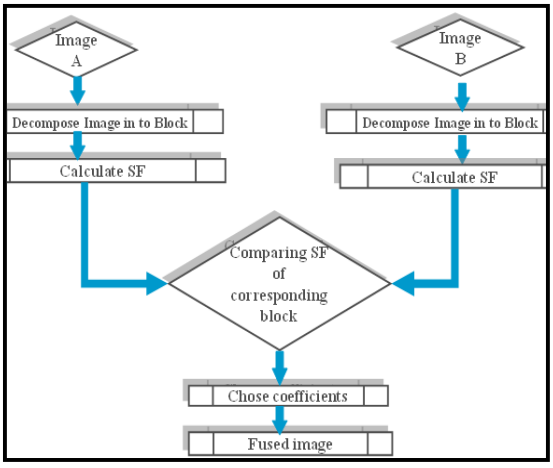

Fig.3 Flow chart of the technique with spatial frequency as a parameter of clarity of images

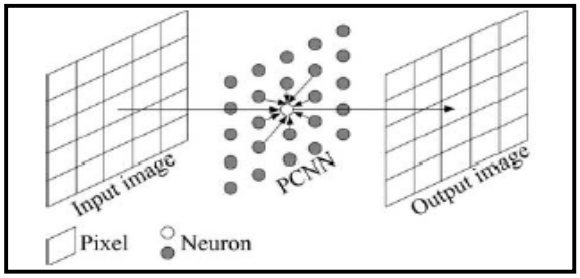

Fig.4 Connection model of PCNN neuron

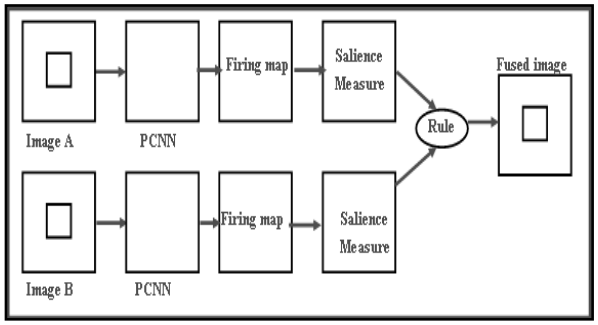

Fig.5 Schematic diagram of PCNN-based fusion algorithm

10.1Image Fusion Algorithm Based on PCNN

PCNN in wavelet domain is utilized as follows:

Step-1: source images are decomposed by *DWT* at the *J-th* scale, and we obtained sub-images at the *J-th* scale.

Step-2: each scale *DWT* coefficients are input to the neurons. There exists a one-to-one correspondence between the coefficients and the network neurons. Each neural cell is connected with neighboring neural cells in linking range, typically within *3×3*(or *5×5*) range.

Step-3: the output of each neuron is calculated by formulas (11)-(15)[14-16], which results in two states, namely firing and non-firing. Then the sum of neuron firing times is counted as formula (16).

$$F_{ij}^{k}(n) = I_{ij}^{k} \tag{11}$$

$$L_{ij}^{k}(n) = e^{-\alpha_L} L_{ij}^{k}(n-1) + V_L \Sigma_{pq} W_{ij,pq} Y_{pq}(n-1) \tag{12}$$

$$U_{ij}^{k}(n) = F_{ij}^{k}(n) * \left(1 + \beta L_{ij}^{k}(n)\right) \tag{13}$$

$$\theta_{ij}^{k}(n) = e^{-\alpha_L} \theta_{ij}^{k}(n-1) + V_\theta Y_{ij}^{k}(n-1) \tag{14}$$

$$Y_{ij}^{k}(n) = \begin{cases} 1 & if\ :\ U_{ij}^{k}(n) > \theta_{ij}^{k}(n) \\ 0 & ,\ otherwise \end{cases} \tag{15}$$

In formulas (11)-(15), the feeding input $F_{ij}^{k}(n)$ is equal to the normalized *DWT* coefficient I_{ij}^{k} corresponding to a pixel in sub-images in wavelet domain, and the linking input $I_{ij}^{k}(n)$ is equal to the sum of neurons firing times in linking range. $W_{ij,pq}$ are the synaptic gain strength. α_L is the decay constants. V_L and V_θ are the amplitude gain. β is the linking strength. $U_{ij}^{k}(n)$ is total internal activity. $\theta_{ij}^{k}(n)$ is the threshold. k denotes the *k-th* sub-image in wavelet domain. Subscripts i, j denote the location of pixel is (i, j) in sub-image and p, q are the size of linking rang in *PCNN*. If $U_{ij}^{k}(n)$ is larger than $\theta_{ij}^{k}(n)$, then the neuron will generate a pulse $Y_{ij}^{k}(n) = 1$, also called one firing times. In fact, sum of $Y_{ij}^{k}(n)$ in n iteration is often defined as formula (16) and used to represent image information. Rather than analyze $Y_{ij}^{k}(n)$, one often analyze $T_{ij}^{k}(n)$ instead. $T_{ij}^{k}(n)$, corresponding to one sub-image, consists firing map whose size is equal to the sub-image and value of each pixel in firing map is equal to value of $T_{ij}^{k}(n)$.

$$T_{ij}^{k}(n) = T_{ij}^{k}(n-1) + Y_{ij}^{k}(n) \tag{16}$$

11. FPGA Implementation of Image Fusion

The *FPGA* is an integrated circuit that contains many (*64* to over *10,000*) identical logic cells that can be viewed as standard components. Each logic cell can independently take on any one of a limited set of personalities. The individual cells are interconnected by a matrix of wires and programmable switches [17]. A user's design is implemented by specifying the simple logic function for each cell and selectively closing the switches in the interconnect matrix. The array of logic cells and interconnects form a fabric of basic building blocks for logic circuits [18]. Field Programmable Gate Arrays *FPGAs* are becoming a critical part of every system design. Many vendors offer many different architectures and processes. The system we have designed consists of the hardware implementation of the *DCT*, *DWT* and *PCNN*-based fusion algorithm the *FPGA* performs wavelet transforms, fusion, and reverse wavelet transforms of the input images. Fig.(6-10) show simple designs of image fusion based on *DCT*, *DWT* and *PCNN*-based that wrote by *VHDL* code [19]. Works are ongoing to design the image fusion modules and the architecture design for these techniques has been implemented on an *Xilinx's Spartan 3AN* board [20].

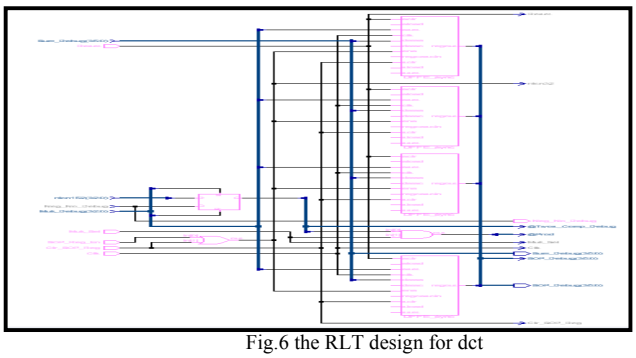

Fig.6 the RLT design for dct

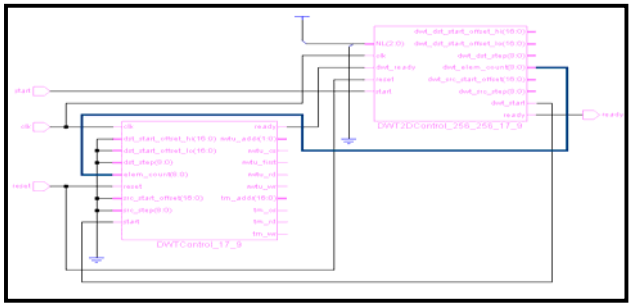

Fig.7 the RLT design for 2d-Dwt

12. Results

The performance of all discussed image fusion techniques has been examined using sets of images; all taken by digital camera (1) "lab" of size *640×480*; (2) "Pepsi" of size *512×512*, and (3) "Toy" of size *512×512*. The objects in Pepsi and Toy images are placed in different distances, thus one object in each image is focused and the other one is blurred. Besides the well-focused image "lab" is used to generate a pair of blurred source images. To perform the blurring process on "Lab" a rotationally symmetric Gaussian low pass filter is used. One object in each image is blurred. Fusion methods are then employed to fuse each pair of the three sets of images. The source images and fusion results for different decomposition levels are illustrated. The performance indices indicate that the image fusion technique based n *DWT* provides the best results among all discussed techniques. Experimental results show that the fusion algorithm is faster than the wavelet based image fusion technique when the images to be saved or transmitted in *JPEG* format. There is no

difference in visual quality between the fused image obtained by this algorithm and that obtained by the wavelet transform based image fusion technique.

13. Conclusion

Along this research, some image fusion approaches have been studied. All of them were found reliable fusion methods in multifocus applications, and in conjunction they gave acceptable results in multi-sensor fusion schemes. As previously mentioned, due to the subjective characteristic of the fusion quality evaluation, it is difficult to conclude which method is the best one for a certain application. For this purpose some psychovisual tests were carried out, where a group of individuals express their subjective preferences between couples of images obtained with different fusion methods. However, the results given by the tests were quite uneven, and no clearly conclusion could be obtained. The implemented algorithms; in the future, have to be implemented using field programmable gate array *(FPGA)* to speed up the performance of fusion process.

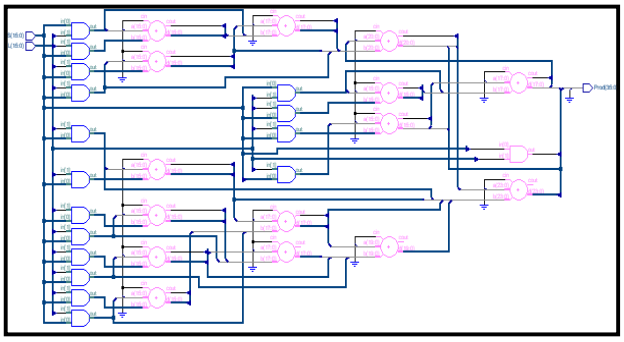

Fig.8 the RLT design for dct multiplier

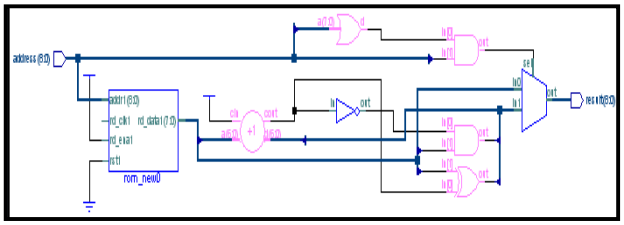

Fig.9 the RLT design for LUT-IDWT

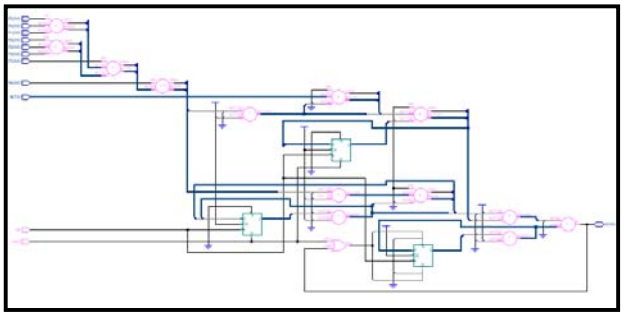

Fig.10 Altera- CycloneII Layout for pcnn RLT design

REFERENCES

[1]. R. Lundqvist; "Atlas-based fusion of medical brain images: methods and applications," PhD dissertation; Uppsala University (Sweden); 2001.

[2]. LehighUniversity,http://www.ece.lehigh.edu/SPCRL/IF/image_fusion.htm.

[3]. J.G. Liu, "Evaluation of Landsat-7 ETM+ Panchromatic Band for Image Fusion with Multi-spectral Bands," Natural Resources Research, Vol. 9, No.4, pp.269-276, Sept 2000.

[4]. A. Morales, T. Charta, S. Ko, ''Morphological pyramids with alternating sequential filters'', IEEE Trans. Image Processing, Vol.4, pp. 965-977, 1995.

[5]. O. Rockinger, T. Fechner, "Pixel-Level Image Fusion: The Case of Image Sequences", Procedings SPIE, Vol. 3374, pp378-388, 1998.

[6]. H. Li, B.S.Manjunath, S. K. Mitra,''Multisensor image fusion using the wavelet transformation'', Graph Models Image Process. Vol.57, pp.235–245, 1995.

[7]. K.R. Rao, and P. Yip, ''Discrete Cosine Transform: Algorithms, Advantages, Applications''. Academic Press, Boston, 1990.

[8]. S. Mallat, "A theory for multiresolution signal decomposition: The wavelet representation," IEEE Trans. Pattern Anal. Machine Intell. Vol.11, pp. 674-693, 1989.

[9]. A.M. Eskicioglu, P.S Fisher, ''Image quality measures and their performance''. IEEE Trans. Comm. Vol.43, No. 12, pp. 2959–2965, 1995.

[10]. J.L. Johnson, M.L Padgett, "PCNN models and applications," IEEE Trans. Neural Networks, Vol.10, pp. 480-498, 1999.

[11]. R.P. Broussard, S.K. Rogers, M.E. Oxley, et al, "Physiologically motivated image fusion for object detection using a pulse coupled neural network,"IEEE Trans. Neural Networks, vol.10, pp. 554-563, 1999.

[12]. Y. Jingwen, Q. Xiaobo, ''Beyond Wavelets and Its Applications'', 1st ed, Ding Fuzhi, Ed. Beijing, China: National Defense Industry Press, 2008.

[13]. B. Xu, Z. Chen, "A multisensor image fusion algorithm based on PCNN", in Proc. of the Fifth World Congress on Intelligent Control and Automation- WCICA' 04,Vol.4, pp. 3679-3682, 2004.

[14]. Q. Xiao-Bo, Y. Jing-Wen, X. Hong-Zhi, Z. Zi-qian, '' Image fusion algorithm based on spatial frequency-motivated Pulse coupled Neural Networks in nonsubsampled contourlet transform domain '',Acta Automatic Sinica, Vol. 34, pp.1508-1514,2008.

[15]. J.M. Kinser: ''Object Isolation Using a Pulse-Coupled Neural Network''. Proc. SPIE 2824,pp. 70–77, 1996.

[16]. J.M. Kinser, ''Pulse-coupled image fusion''. Opt. Eng, Vol. 36, No. 3, pp. 737–742 ,1997.

[17]. http://en.wikipedia.org/wiki/Field_programmable_gate_array#cite_note-history-1.

[18]. N. Lalle ASIC Corporation, ''FPGA Judgment Day: Rise of Second Generation Structured ASICs''. March, 2008. Retrieved February 5, 2009.

[19]. P. J. Ashenden, "The Student's Guide to VHDL," Morgan Kaufmann Publishers, Inc, San Francisco, 1998.

[20]. http://www.xilinx.com/company/gettingstarted/fpgavsasic.htm.

Table:1 Measured entropy of fused images by average; PCA, and Modified DCT

Source Images	Average	PCA	Modified DCT
Lab 1	6.8756	6.8756	6.8756
Lab 2	6.9302	6.9302	6.9302
Fused image	4.8925	6.9658	6.9529

Table:2 Measured RMSE, MSE of fused images by average PCA and Modified DCT

	Average	PCA	Modified DCT
RMSE	12.7468	12.3135	12.4987
MSE	162.4801	151.6234	156.2169

Table: 3 Measured SNR, PSNR of fused images by average PCA and Modified DCT

	Average	PCA	Modified DCT
SNR(db)	0.1173	0.2737	0.1162
PSNR(db)	6.0228	26.3231	0.1162

Table: 4 measured entropy of fused images by LPT, gradient, morphological. 'Lab' of size 640×480

Level number	LPT	Gradient	Morphological
1	7.0014	6.9291	7.0699
2	7.0277	6.9435	7.0862
3	7.0514	6.9555	7.0729

Table: 5A Measured RMSE of fused images by LPT, morphological and gradient 'lab' of size 640×480

Level number	LPT	Gradient	Morphological
1	12.4967	12.5415	12.5713
2	12.4919	12.5455	12.6022
3	12.4915	12.5359	12.6039

Table: 5B Measured MSE of fused images by LPT, morphological and gradient 'lab' of size 640×480

Level number	LPT	Gradient	Morphological
1	156.1678	157.2896	158.0381
2	156.0470	157.3885	158.8146
3	156.0383	157.1496	158.8578

Table: 6A measured SNR (db) of fused images by LPT, Morphological and gradient

Level number	LPT	Gradient	Morphological
1	0.1130	0.1090	0.0840
2	0.1045	0.1123	0.0520
3	0.0939	0.1195	0.0430

Table: 6B measured PSNR (db) of fused images by LPT, Morphological and gradient

Level number	LPT	Gradient	Morphological
1	26.1949	26.1638	26.1432
2	26.1982	26.1611	26.1219
3	26.1985	26.1677	26.1207

Table: 7 measured entropy of fused images by DWT & LPT' Pepsi'. Of size 512×512. Entropy of I1=7.0880 and I2=7.1085

Level number	DWT	LPT	Level number
1	7.1326	7.1139	1
2	7.1558	7.1146	2
3	7.1590	7.1279	3

Table: 8 measuring the Entropy, MSE and PSNR of DWT, LPT and SF technique

	Entropy	MSE	PSNR(db)
DWT(*db2*)(min, min)	6.9315	160.0265	26.0889
DWT(*bior3.7*)(max ,max)	7.0223	147.9140	26.4307
LPT	7.0014	156.1678	26.1949
SF	6.9576	12.5020	26.1995

Table:9 measured Entropy of fused (Toy) images by PCNN+DWT &DWT

Algorithm	Entropy	Algorithm	Entropy
PCNN+DWT	7.6923	PCNN+DWT	7.6923
DWT	6.8526	DWT	6.8526

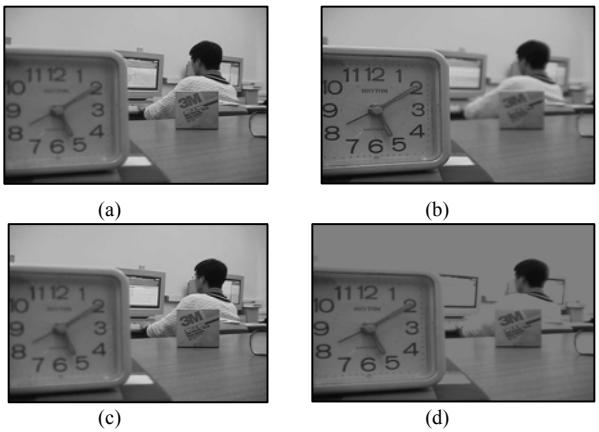

(a) (b) (c) (d)

Fig.11 (a) reference image (everywhere-in-focus) (b) and (c) Blurred images in left and right (d) fused image by average

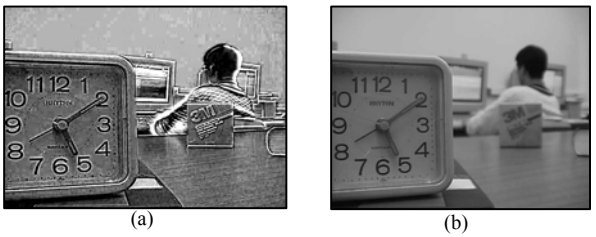

(a) (b)

Fig.12 (a) fused image by PCA (b) Fused image by Modified DCT

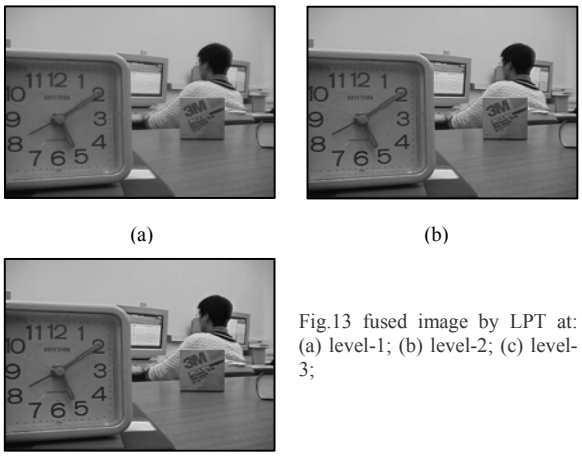

(a) (b) (c)

Fig.13 fused image by LPT at: (a) level-1; (b) level-2; (c) level-3;

(a) (b)

Fig.14 fused image by morphological method at: (a) level-1; (b) level-2; (c) level-3;

(a) (b)

Fig.15 Fused images by gradient pyramid at: (a) level-1; (b) level-2; (c) level-3

(c)

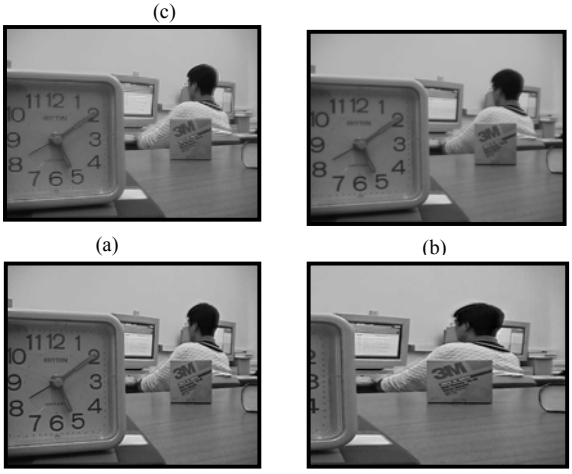

(a) (b)

(c) (d)

Fig.16 Lab images fusion results. (a), (b) Fused image using DWT (c) fused image using LPT. (c) Fused image using SF

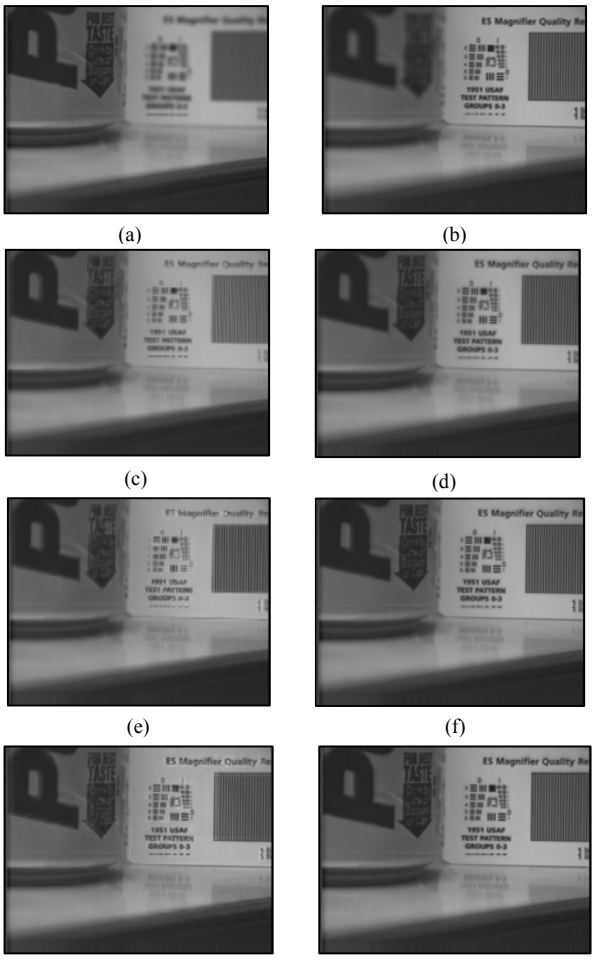

(a) (b)

(c) (d)

(e) (f)

(g) (h)

Fig.17 (a, and b) Blurred images in left and right; (c, and d) Fused image by DWT at level-1, fused image by LPT at level 1(e, and f) Fused image by DWT at level-2, fused image by LPT at level-2 (g, and h) Fused image by DWT at level-3, fused image by LPT at level-3

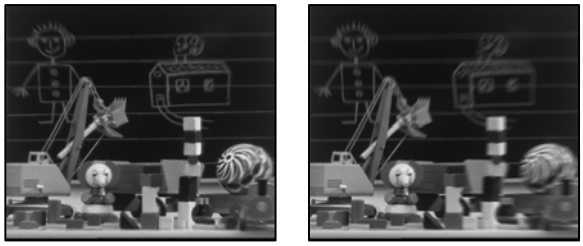

(a) (b)

Fig. 18 The ‘‘Toy’’ images source and fusion image (a) source focus on the right (b) focus on left (c) fused image using PCNN+DWT

(c)